ELSEVIER

Surface Science 417 (1998) 169–188

surface science

Cycloaddition reactions of unsaturated hydrocarbons on the Si(100)-(2 × 1) surface: theoretical predictions

R. Konečný [1], D.J. Doren *

Department of Chemistry and Biochemistry, University of Delaware, Newark, DE 19716, USA

Received 11 March 1998; accepted for publication 22 June 1998

Abstract

First-principles electronic structure calculations have been used to study the structure, energetics and vibrational spectra of the chemisorption products of several unsaturated hydrocarbons on the Si(100)-(2 × 1) surface. The calculations use a hybrid non-local density functional theory and a cluster model of the surface. Ethylene and acetylene react by a $[2_s+2_s]$ cycloaddition mechanism. Conjugated dienes (1,3-cyclohexadiene, 1,3-butadiene, 2,3-dimethyl-1,3-butadiene) and benzene can also react by a novel $[4_s+2_s]$ cycloaddition, or Diels–Alder mechanism. For each diene, the Diels–Alder product is energetically favored over the more strained $[2_s+2_s]$ product. The reaction mechanism for Diels–Alder addition, other competing reactions, and the effects of post-hydrogenation are all discussed. Comparisons to experimental observations are made throughout.

Keywords: Alkenes; Alkynes; Aromatics; Density functional calculations; Dienes; Silicon; Surface chemical reaction

1. Introduction

Reactions of hydrocarbon molecules with silicon surfaces have a wide variety of potential applications in materials chemistry. Unsaturated hydrocarbons are used as precursor molecules for chemical vapor deposition (CVD) of silicon carbide and diamond-like films on silicon surfaces. Hydrocarbon films may be useful as low dielectric materials for microelectronics, and would be especially useful if such films can form covalent bonds to the surface that chemically and electrically passivate the surface. Covalently bound organic monolayers may serve as an interface between silicon and other organic materials, particularly if monolayers with a variety of chemical functionality can be produced. Coupling of silicon-based materials to organic materials is likely to be useful in nonlinear optical materials, optoelectronies, sensors, low dielectric materials, lithography, and molecular electronics.

Motivated primarily by CVD applications, there have been many studies of small hydrocarbon. adsorption on Si(100) [1]. Most of this work has concerned ethylene and acetylene, though recently many other unsaturated hydrocarbons have been studied. While alkanes do not react on the clean Si(100) surface, unsaturated hydrocarbons havea high chemisorption probability [2–5]. Spectroscopic evidence indicates that π-bonds in alkenes and alkynes react readily with the surface

* Corresponding author. Fax: +1 302 831 6335; e-mail: doren@udel.edu

[1] Current address: Department of Chemistry, Cornell University, Baker Laboratory, Ithaca, NY 14853-1301, USA.

0039-6028/98/$ – see front matter
PII: S0039-6028(98)00554-8

dangling bonds to form a pair of C–Si σ-bonds [6–9]. Other molecules containing π-bonds appear to react in a similar way on Si(100) [2,10,11] and even benzene will chemisorb in a di-σ bonded configuration on the (100) surface [12–14].

There has been little work on formation of well-defined organic layers on the Si(100) surface, despite the potential technological applications. Linford et al. [15] prepared alkyl monolayers on hydrogen-terminated Si(111) surface from 1-alkenes using a free-radical mechanism. Hamers et al. [10] reported formation of monolayers of cyclopentene on the Si(100) surface. Scanning tunneling microscopy (STM) and infrared spectroscopy show that these layers are ordered both translationally and rotationally and exhibit measurable anisotropy in optical properties.

We have recently described a novel surface reaction that may be useful in forming covalently bound organic layers on the Si(100) surface, the surface analog of the classic Diels–Alder (DA) reaction [16]. The weak π-bond between the dangling bonds of the surface dimer can act as a dienophile in a reaction with a conjugated diene, as illustrated in Fig. 1 with 1,3-cyclohexadiene as a prototypical diene. Other conjugated dienes, such as 1,3-butadiene or substituted dienes, go through analogous reactions, so that a wide variety of organic monolayers can be produced from this reaction. The product of this cycloaddition reaction suggests novel applications, since it saturates the surface dangling bonds while retaining the potential for further controlled chemical modification at the carbon–carbon double bond.

In this paper we describe and compare the thermodynamics of chemisorption for a variety of unsaturated hydrocarbons. In Section 2 we discuss adsorption of ethylene and acetylene, which can undergo $[2_s+2_s]$ cycloaddition to form products with two Si–C bonds in a four-member ring. These products have molecular analogs that have been structurally characterized, providing some further insight into the surface reaction and allowing tests of the accuracy of our electronic structure methods. Section 3 concerns adsorption of conjugated dienes. In addition to the $[2_s+2_s]$ cycloaddition, these molecules can react by the Diels–Alder mechanism, a $[4_s+2_s]$ cycloaddition. This latter reaction results in a six-member ring with two C–Si σ-bonds. The mechanism and activation energy of the Diels–Alder reaction are also discussed. Some alkenes can also undergo the ene reaction, which yields a product with one C–Si bond and a H–Si bond. This reaction is illustrated for 1,3-cyclohexadiene, and the reaction energy is compared with that of the $[2_s+2_s]$ and $[4_s+2_s]$ cycloadditions. We then turn to chemisorption of benzene, where both $[2_s+2_s]$ and $[4_s+2_s]$ cycloaddition products are possible, but more weakly bound than the corresponding products of nonaromatic dienes. Several experimental groups have exposed hydrocarbon adsorbates to atomic hydrogen as a tool for analyzing hydrocarbon adsorption products. We show in Section 3 that post-hydrogenation can cause isomerization of the adsorbate complex, complicating the interpretation of experimental results. The concluding discussion includes a guide for qualitative predictions of the relative energetics for the different reactions.

2. Theoretical models and methods

The calculations reported in this paper have been carried out using density functional theory with the B3LYP functional [17,18] and split-

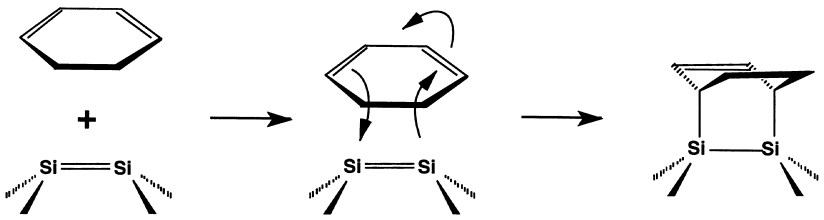

Fig. 1. Schematic mechanism of the surface Diels–Alder reaction.

valence 6-31G** or 6-31G* basis sets [19]. Some additional calculations have been also performed with the more extensive 6-311G** basis set [19]. Energy and derivative calculations have been carried out with the Gaussian 94 series of programs [19].

A Si_9H_9 cluster has been used to model the surface. This is the smallest cluster that can represent a realistic Si(100)-(2×1) surface without artificial geometric constraints. Bonds to sub-surface silicon atoms are terminated with hydrogen atoms. This cluster model gives energetic and geometric predictions in good agreement with experiment and other theoretical methods at reasonable computational cost, though it neglects interactions with adjacent dimers [20,21]

The properties of critical points of the potential surface have been determined by optimizing the cluster model (without constraints), and characterized by computing the second derivative matrix. Reported vibrational frequencies have been calculated at the B3LYP/6-31G* level using fully optimized B3LYP/6-31G* geometries. The reported frequencies have been scaled by a factor of 0.94 [22].

3. Results and discussion

3.1. Ethylene and acetylene

It is known experimentally that alkenes and alkynes chemisorb readily on Si(100) [1,6,10,11] though there has been some controversy about the structure of the product. One possible reaction of a C–C π-bond with the Si(100) surface dimers is a $[2_s+2_s]$ cycloaddition, leaving the surface dimer bond intact. However, a variety of experimental observations have been interpreted as evidence that ethylene adsorbs by insertion into the dimer, cleaving the dimer bond and leaving two dangling bonds on each dimer [4,7,8]. Theoretical calculations have called the initial interpretation of the experiments into question [23–28]. First-principles calculations support the $[2_s+2_s]$ cycloaddition (with an intact dimer bond) as the energetically favored product of ethylene or acetylene adsorption [25–28]. We provide additional evidence here that the cycloaddition product is the result of ethylene or acetylene adsorption. Some further comparisons to experimental work are made in Section 3.3.2.

We find that the lowest energy non-dissociative chemisorption products of ethylene and acetylene on the Si(100) surface are the $[2_s+2_s]$ cycloaddition products with intact dimer bonds. The energy-minimized structures, optimized at the B3LYP/6-31G* level, are shown in Fig. 2. The geometric and energetic parameters are summarized in Table 1. We have also performed a full optimization of these complexes using the more extensive 6-311G** basis set with the B3LYP functional, but there were no significant changes in geometry: bond lengths predicted with the two bases differ by no more than 0.01 Å and bond angles differ by no more than 1°. The calculated adsorption energies are lower at the B3LYP/6-311G** level (Table 1). This is not surprising, since large basis sets tend to converge to lower reaction energies.

The predicted structure resulting from ethylene chemisorption has two Si–C σ-bonds and an intact Si–Si dimer bond. The ethylene C–C bond stretches upon adsorption to 1.57 Å (compared with 1.34 Å in molecular ethylene). The longer bond results primarily from rehybridization as the C–C bond changes from a double bond to a single bond; the product C–C bond length is only slightly longer than the C–C bond in ethane (1.54 Å). The Si–Si–C angle (78.4°) is far from the tetrahedral value and indicates significant ring strain. In response to this strain, the Si–Si–C–C ring in the ethylene adsorbate complex puckers slightly (Si–Si–C–C dihedral angle = 7.4°). The Si–Si dimer bond is 2.36 Å which is slightly shorter than the dimer on the monohydride surface (2.39 Å according to B3LYP/6-31G* calculations). The reaction energy for adsorption of ethylene on the Si(100) surface is -43.2 kcal mol^{-1} with the largest basis set. The experimental estimate of the desorption energy (from temperature programmed desorption) is -38.0 kcal mol^{-1} [4]. Agreement between the theoretical prediction and experiment is reasonable, though far from perfect. The difference probably results from several sources: aside from experimental uncertainty, the cluster model

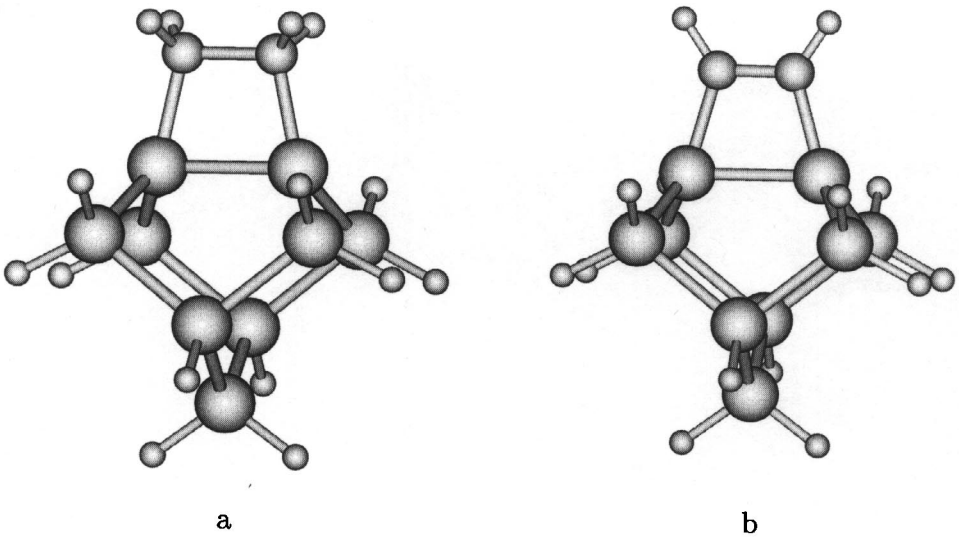

Fig. 2. B3LYP/6-31G* optimized product geometries of adsorption of: (a) ethylene; and (b) acetylene on Si(100) surface.

Table 1
Structural parameters for products of adsorption of acetylene and ethylene on the Si(100) surface as calculated at the B3LYP/6-31G* level. Adsorption energies are also reported for B3LYP/6-311G** level

	Ethylene	Acetylene
Si–Si (Å)	2.360	2.368
Si–C (Å)	1.953	1.909
C–C (Å)	1.570	1.353
Si–C–C (°)	101.4	105.5
Si–Si–C (°)	78.2	74.4
Si–Si–C–C (°)	7.4	0.0
ΔE (kcal mol^{-1}) (B3LYP/6-31G*)	−45.7	−66.1
ΔE (kcal mol^{-1}) (B3LYP/6-311G**)	−43.2	−60.2
ΔE (kcal mol^{-1}) (Experiment)	-38.0 ± 1.5[4]	-46.1 ± 2.0[a,5]

[a] See discussion about this value in the text.

used here does not completely account for the stabilization of the bare surface by buckling and the basis set is probably not completely converged (correcting each of these errors would make the predicted reaction energy less negative). There have also been other theoretical predictions of the reaction energy: Fisher et al. obtained −36.2 kcal mol^{-1} [27] and Pan et al. obtained −41.7 kcal mol^{-1} [28], using periodic slab models. Detailed comparisons of the various theoretical predictions are not possible as they were all obtained with different DFT methods. Of these predictions, only the present ones include gradient corrections to DFT self-consistently. The present calculations are the only ones that predict a non-planar Si–Si–C–C ring, though there is experimental evidence for an adsorbate configuration with local C_1 symmetry [6,9].

Similar to ethylene, acetylene forms a di-σ bonded adsorbate complex on the Si(100) surface, though the acetylene product retains a C–C double bond (Table 1). The C–C bond length in the adsorbate complex is typical of a double bond (1.35 Å compared with 1.34 Å in ethylene) and the Si–Si bond distance is slightly shorter than on the monohydride surface (2.37 Å). The Si–Si–C and Si–C–C ring angles are farther from their optimal values (109.5° and 120°, respectively) than in the ethylene complex. In contrast to ethylene, the Si–Si–C–C ring is planar and the product has C_{2v} symmetry. Again, there is some experimental evidence in favor of a structure with local C_1 symmetry [3,9] though in our calculations, explicit searches for low symmetry minima always led back to the C_{2v} structure. As shown below, the difference in ring twisting predicted for the two surface complexes is also seen in the predicted and experi-

mental structure of two molecular analogs, so the difference has verified precedents which are reproduced by theory. More detailed comparisons of theory and experiment will be needed to resolve the apparent differences between the predicted and observed structural properties of the acetylene complex. The calculated adsorption energy for acetylene is -66.1 kcal mol^{-1} (B3LYP/6-31G*), far from the reported experimental value of -46.1 kcal mol^{-1} [5]. However, the measured value is obtained from a thermal desorption experiment, in which only a few percent of a monolayer of acetylene desorbs, while the majority decomposes. It is likely that this experiment is not an accurate probe of the majority-species binding energy.

The difference in calculated binding energy for ethylene and acetylene is 20 kcal mol^{-1} with the 6-31G* basis (17 kcal mol^{-1} with the 6-311G** basis). This is a consequence of two effects: the π-bonds are weaker in acetylene than ethylene, and bonds to sp^2 carbon (as in the acetylene complex) are stronger than bonds to sp^3 carbon (as in the ethylene complex). The shorter, stronger Si–C bonds in acetylene reflect the greater contribution of the carbon s orbitals (relative to carbon p orbitals) to the bonding orbital. In Section 3.1.1, we study molecular analogs of these surface complexes and show that there is no substantial difference in ring strain in the ethylene and acetylene complexes.

We have searched for energy minima corresponding to di-σ bonded complexes with a cleaved Si–Si dimer bond by starting optimizations with the Si–Si bond stretched to 4.0 Å (the Si–Si distance in the unreconstructed ideal surface is 3.84 Å) [29]. No minima near this starting configuration were found, and geometry searches for both ethylene and acetylene led back to the adsorbate complexes described above, with intact Si–Si dimer bonds. Other theoretical studies have also concluded that there is no stable minimum corresponding to a broken Si–Si dimer bond [25–28].

We have not calculated the reaction path for ethylene or acetylene adsorption. The $[2_s+2_s]$ cycloaddition reaction is orbital symmetry forbidden (Fig. 3a) and, according to the Woodward–Hoffmann rules [30], is expected to have a high activation barrier on a symmetric reaction path. The observation that chemisorption is facile suggests that the reaction path is nonsymmetric, involving a buckled surface dimer. Although it is useful to think of the interaction between dangling bonds on the Si(100)-(2×1) surface as a weak π-bond, the thermal $[2_s+2_s]$ cycloaddition that occurs so readily on the surface is not feasible for a typical C–C π-bond. The facile nature of the $[2_s+2_s]$ addition on the Si(100) surface illustrates the high reactivity of this surface, a consequence of the fact that surface dangling bonds interact weakly rather than forming a strong π-bond.

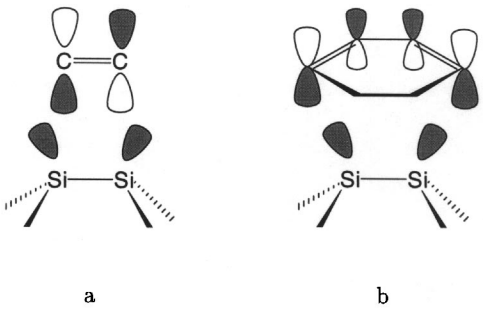

Fig. 3. Schematic picture of highest occupied molecular orbital (HOMO) of the surface and lowest occupied molecular orbital (LUMO) of: (a) the ethylene; and (b) 1,3-cyclohexadiene.

3.1.1. Molecular analogs of the surface $[2_s+2_s]$ addition complexes

Cycloadditions of ethylene and acetylene to disilene (Si_2H_4) yield molecular analogs of the surface complexes described above. The products of these reactions are 1,2-disilacyclobutane ($C_2Si_2H_8$) and 1,2-disilacyclobut-3-ene ($C_2Si_2H_6$). We have performed full optimizations of these molecules to make comparisons between Si(100) surface chemistry and molecular chemistry of the Si–Si double bond [31,32]. These calculations also permit calibration of our theoretical methods since X-ray diffraction structures have been determined for a substituted disilacyclobutane [33] and a substituted disilacyclobutene [34]. The structural predictions for the $C_2Si_2H_8$ and $C_2Si_2H_6$ molecules, together with measured values for the substituted molecules are presented in Table 2. There is good agreement between the calculated and experimen-

Table 2
Structural parameters and reaction energy for products of adsorption of acetylene and ethylene on the Si(100) surface as calculated at the B3LYP/6-31G* level

	1,2-disilacyclobutane		1,2-disilacyclobut-3-ene	
	Calc.	Exp.[a]	Calc.	Exp.[b]
Si–Si (Å)	2.343	2.344	2.349	2.359
Si–C (Å)	1.928	1.932	1.894	1.882
C–C (Å)	1.567	1.463	1.357	1.357
Si–C–C (°)	99.1	100.3	101.5	105.4
Si–Si–C (°)	76.7	75.1	78.5	74.5
Si–Si–C–C (°)	26.2	21.6	0.0	0.0
ΔE (kcal mol^{-1}) (B3LYP/6-31G*)	−49.7		−70.6	

[a] X-ray determined (Ref. [33]) geometry of 1, 1,2,2-tetraphenyl-3,4-bis[bis(trimethylsilyl) methylene]-1,2-disilacyclobutane.
[b] X-ray determined (Ref. [34]) geometry of 9,9,10,10-tetrakis[2-(dimethylaminomethyl)phenyl]-9,10-disilabicyclo[6.2.0]dec-1(8)-ene.

tal geometries, with the only substantial difference being in the value of the C–C bond length in 1,2-disilacyclobutane. This can be attributed to electronic and steric effects of substituents on the Si–Si–C–C ring in the experimental structure that were not included in the calculated molecule.

The calculated bond lengths and bond angles for $C_2Si_2H_8$ and $C_2Si_2H_6$ are very similar to those of the corresponding surface complexes. In particular, the Si–Si–C–C ring is nonplanar in $C_2Si_2H_8$ (the analog of adsorbed ethylene) while the ring is planar in $C_2Si_2H_6$ (the analog of adsorbed acetylene). If out-of-plane twisting relieves ring strain in species with C–C single bonds, it appears that there is no energetic advantage to twisting species with a C–C double bond, reflecting the differences in hybridization in the two cases. The most significant difference between the molecules and their surface analogs is that the Si–Si–C–C ring in 1,2-disilacyclobutane is twisted out of plane, with a larger dihedral angle than the twisted ethylene adsorbate complex on Si(100). To determine the reduction in strain energy that results from twisting the ring, we have optimized 1,2-disilacyclobutane with C_{2v} symmetry, where the Si–Si–C–C ring is constrained to lie in a plane. The constrained molecule is only 1.1 kcal mol^{-1} (B3LYP/6-31G*) higher in energy than the unconstrained molecule with the twisted ring, so the energetic effect of ring twisting in the molecule is small. Moreover, this result indicates that the difference in dihedral angles in the molecular model and surface adsorbate complex is not energetically significant. The calculated reaction energies for the $[2_s+2_s]$ cycloadditions of ethylene and acetylene to disilene (Table 2) are only slightly more favorable (by 4 kcal mol^{-1}) than for the corresponding surface reactions (Table 1). Given the similar geometries and reaction energies of the surface complexes and their molecular analogs, it appears that the strain is similar in the two environments.

Since the difference in reaction energy between the two molecular reactions is nearly the same as that between the corresponding surface reactions, the molecules make a convenient model for understanding the origins of this energy difference. An estimate of the difference in reaction energies can be reached by comparing heats of reaction from group additivity arguments [35]. Walsh [36] has determined the group contribution to heats of formation for Si(C)$_2$(H) (a Si bound to two Cs and a H) and Benson [35] gives a value for C$_d$(C)(H) (a C that participates in a double bond and is also bound to a C and a H). These values can be taken as estimates for Si(C)(Si)(H) and C$_d$(Si)(H), respectively. The resulting predictions for heats of formation are −12.5 kcal mol^{-1} for the ethylene complex ($C_2Si_2H_8$) and +12.8 kcal mol^{-1} for the acetylene complex ($C_2Si_2H_6$). Comparison to the heats of formation for ethylene, acetylene and disilene (+12.5, +54.0 and +66.2 kcal mol^{-1}, respectively) shows that the heats of reaction for the $[2_s+2_s]$ cycloadditions to disilene are −91.2 kcal mol^{-1} for ethylene and

-107.4 kcal mol^{-1} for acetylene. The difference in heats of reaction, 16.2 kcal mol^{-1}, is close to the difference in reaction energies for the surface cycloadditions. In the group additivity calculation, no corrections for ring strain or other effects have been included. Thus, ring strain does not need to be invoked to account for the the difference in heat of reaction for ethylene and acetylene. Instead, this difference must be due to differences in the group contributions in the reactants and products. These differences in group contributions correspond to differences in the π-bond strength in ethylene and acetylene, and differences in the strength of Si–C bonds for singly and doubly bonded carbons, the same effects noted in Section 3.1.

3.2. Diels–Alder addition

The Diels–Alder reaction is a $[4_s+2_s]$ cycloaddition between a conjugated diene and a ''dienophile'', which in this case is the Si(100) surface dimer (Fig. 1). The product has a cyclic structure, with the organic molecule bound to the surface by two Si–C bonds. There is a C–C double bond in the product which may also allow further controlled chemistry on the surface. The initial discussion here uses 1,3-cyclohexadiene as a prototype because its cyclic structure allows only one conformational isomer, and only one stereoisomer is possible in the product. The structure and energetics of the Diels–Alder product are discussed and compared with products of some other possible reactions. This is followed by a description of the reaction mechanism and activation energy. Next we turn to reactions of other dienes.

Since the assignment of vibrational spectra for chemisorbed cyclohexadiene is not as simple as for some other dienes, the first experimental studies of the Diels–Alder reaction on Si(100) have been done with 1,3-butadiene and 2,4-dimethyl-1,3-butadiene, so we have included a discussion of the adsorption products of these molecules. Finally, there is experimental evidence that benzene chemisorbs on Si(100), and we explore the possibility that this reaction is also of the Diels–Alder type.

3.2.1. 1,3-Cyclohexadiene

We have optimized the product of a Diels–Alder reaction (the $[4_s+2_s]$ product) between 1,3-cyclohexadiene and the Si(100)-(2×1) surface dimer at the B3LYP/6-31G** level. This nondissociative adsorption reaction forms two new Si–C bonds and one C–C π-bond, while simultaneously breaking the weak surface Si–Si π-bond and two C–C π-bonds in the alkene (Fig. 4). The calculated adsorption energy is -54.0 kcal mol^{-1}.

Structural data for the $[4_s+2_s]$ adsorbate complex are presented in Table 3. The Si–Si bond is stretched upon adsorption to 2.37 Å [compared with 2.22 Å on the bare Si(100) surface]. This is again slightly shorter than the similar Si–Si bond in a monohydride on the Si(100) surface (2.39 Å). The Si–C distances are 1.95 Å, similar to the Si–C bond lengths in ethylene and acetylene adsorption products on Si(100) and their molecular analogs (Tables 1 and 2). The Si–Si–C angle (96.6°) is smaller than the ideal tetrahedral value, although this angle is less distorted than similar angles in the ethylene or acetylene adsorption complexes (Table 1). The B3LYP/6-31G* calculated vibrational frequencies in the C–H stretching region for the $[4_s+2_s]$ product are reported in Table 4.

The Diels–Alder reaction is not the only mechanism by which 1,3-cyclohexadiene can react with the Si(100) surface. Similar to the surface reaction with ethylene, dienes can adsorb on the surface in a $[2_s+2_s]$ fashion, involving only one carbon–carbon π-bond. Indeed, in analogous disilene reactions, the Si–Si double bond preferentially reacts with dienes by the $[2_s+2_s]$ mechanism: when simple conjugated dienes are exposed to disilenes, the $[4_s+2_s]$ product is not found [31,32].

We have optimized the $[2_s+2_s]$ cycloaddition product of 1,3-cyclohexadiene on the Si(100) surface. The structure of the adsorbate complex is depicted in Fig. 5. Structural data are presented in Table 3. The Si–Si bond is shorter than in the $[4_s+2_s]$ complex, indicating greater ring strain. One of the Si–C–C angles (121.8°) is distorted from the optimal tetrahedral configuration, as are the Si–Si–C angles (78.1°, 77.9°). Judging from these values and from the twisted Si–Si–C–C ring (Fig. 5), the ring strain in the $[2_s+2_s]$ product is more severe than in the $[4_s+2_s]$ product. Note that

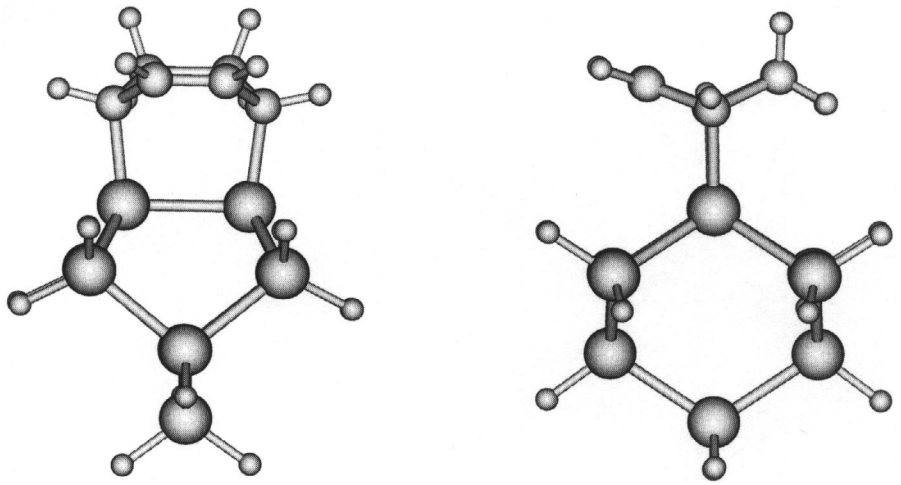

Fig. 4. Product of 1,3-cyclohexadiene adsorption on the Si(100) surface through Diels–Alder mechanism as calculated at the B3LYP/6-31G** level. A view along the [1$\bar{1}$0] and [110] directions.

Table 3
Structural parameters for products of adsorption of 1,3-cyclohexadiene on Si(100) surface as calculated at the B3LYP/6-31G** level and reaction energies with several basis sets

	$[4_s+2_s]$ complex	$[2_s+2_s]$ complex
Si–Si (Å)	2.373	2.353
Si–C (Å)	1.953	1.965, 1.975
C–C (Å)	2.823[a]	1.576
Si–C–C (°)	109.7, 105.4	121.8, 110.0
Si–Si–C (°)	96.6	78.1, 77.9
Si–C–H (°)	110.5	111.9, 103.0
ΔE (kcal mol^{-1}) (B3LYP/6-31G*)	−54.1	−38.8
ΔE (kcal mol^{-1}) (B3LYP/6-31G**)	−54.0	−38.8
ΔE (kcal mol^{-1}) (B3LYP/6-311G**)	−52.6	−37.1

[a] Distance across the ring, between two carbons bonded to silicon atoms.

Table 4
The calculated vibrational frequencies for the $[4_s+2_s]$, and $[2_s+2_s]$ cycloaddition adducts o£ 1,3-cyclohexadiene

	Group	Symmetry	Frequency (cm^{-1})
$[4_s+2_s]$			
	–CH_2–	a	2859
	–CH_2–	s	2872
	–CH_2–	a	2888
	–CH–	a	2896
	–CH–	s	2897
	–CH_2–	s	2909
	–CH=CH–	a	2983
	–CH=CH–	s	3003
$[2_s+2_s]$			
	–CH_2–	s	2832
	–CH_2–	a	2838
		s	2841
	–CH–, –CH_2–		
		a	2858
	–CH–, –CH_2–		
	–CH_2–	a	2872
	–CH_2–	s	2888
	–CH=CH–	a	2958
	–CH=CH–	s	2981

the ethylene addition product is more strongly bound (by about 5 kcal mol^{-1}) than the analogous $[2_s+2_s]$ cyclohexadiene adsorption complex. This difference can be attributed to the loss of resonance energy in the reaction of the conjugated diene.

The energy of the $[2_s+2_s]$ complex is 15.2 kcal mol^{-1} higher than the energy of the $[4_s+2_s]$ complex, so the $[4_s+2_s]$ product is thermodynamically preferred. The energy difference between these products can be attributed entirely to the difference in ring strain. A group additivity approach would predict that both products should have the same energy (although actual values for

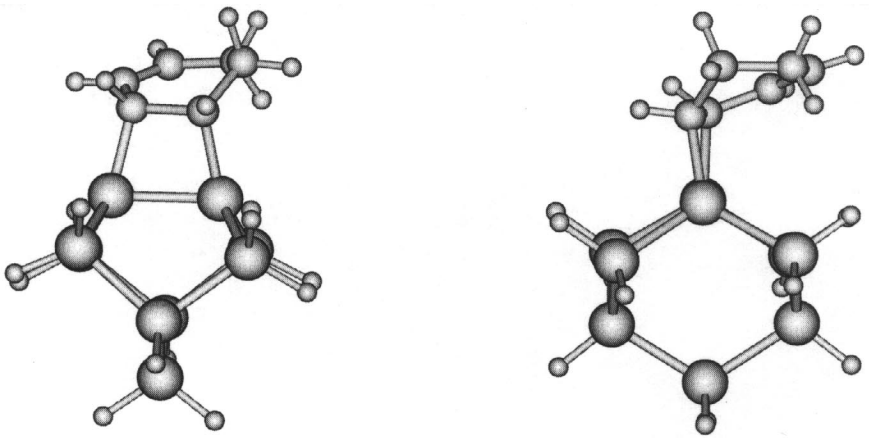

Fig. 5. Fully optimized geometry of the product $[2_s+2_s]$ cycloaddition of 1,3-cyclohexadiene on the Si(100) surface as calculated at the B3LYP/6-31G** level. A view along the $[1\bar{1}0]$ and [110] directions.

group contributions are not available, the same groups are present in both molecules). If the strain energy is taken as the difference between the actual heat of formation and the heat of formation predicted from group additivity [35], then the difference in stability of these two products is necessarily a difference in strain energy.

As a further test of the basis sets used, we have also carried out a full optimization of the $[4_s+2_s]$ and $[2_s+2_s]$ products with different size basis sets. Specifically, we have used the 6-31G* basis and the triple-zeta 6-311G** basis. The geometric parameters of the calculated complexes did not change significantly (they agree within 0.01 Å and 1°), nor did the adsorption energies (Table 3). Overall, these calculations provide strong evidence that the Diels–Alder product is more stable than the $[2_s+2_s]$ addition product. The result that the four-membered ring in the $[2_s+2_s]$ product has 15 kcal mol^{-1} more ring strain than the six-membered rings in the $[4_s+2_s]$ product is completely consistent with chemical experience. The B3LYP functional is generally reliable for predicting bond energies to within a few kcal mol^{-1}, which is much smaller than the energy difference calculated here. Moreover, the $[4_s+2_s]$ and $[2_s+2_s]$ products are isomers related by an isodesmic reaction (the two isomers have the same number of the same types of bonds). Energy differences calculated for isodesmic reactions are more reliable than for general reactions. Thus, we predict with a high degree of confidence that the $[4_s+2_s]$ addition product is more thermodynamically stable than the $[2_s+2_s]$ product.

The B3LYP/6-31G* calculated vibrational frequencies for the $[2_s+2_s1$ adduct are reported in Table 4. The most notable difference between the vibrational spectra of the $[4_s+2_s]$ and $[2_s+2_s1$ products is that the range of the C–H stretch region for the $[4_s+2_s]$ product (2859–3003 cm^{-1}) is shifted higher than the range for the $[2_s+2_s]$ product (2832–2981 cm^{-1}).

While $[2_s+2_s]$ cycloaddition may compete with the Diels–Alder addition for any 1,3-diene, in the case of cyclohexadiene there is also another potential competing reaction, the "ene" reaction (Fig. 6). The reaction energy for the ene reaction is -43.64 kcal mol^{-1} (B3LYP/6-31G**), making this product 4.8 kcal mol^{-1} more stable than the $[2_s+2_s]$ addition product, but 10.4 kcal mol^{-1} less stable then the $[4_s+2_s]$ product. The reaction requires breaking a C–H bond, so it is likely to

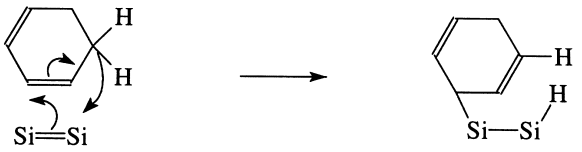

Fig. 6. Schematic mechanism of the surface ene reaction.

have a significant activation barrier. In any case, these calculations predict that the Diels–Alder product is lower in energy than either of the alternative reactions.

Recent STM studies of 1,3-cyclohexadiene adsorbed on Si(100) show that two different products are formed, and the images are consistent with these being the $[4_s+2_s]$ and $[2_s+2_s]$ species [37]. Given the difference in energy between these two products, this observation implies that the two reactions compete kinetically, but that the thermodynamic product distribution has not been reached. It may be possible to obtain a surface with only the thermodynamically favored Diels–Alder product by annealing the initially formed product distribution, or by desorbing the weakly bound $[2_s+2_s]$ product and readsorbing additional cyclohexadiene.

3.2.2. Reaction pathways of surface Diels–Alder reaction

The Diels–Alder reaction is the most widely used and best known pericyclic reaction. Despite a long history of experimental [38–40] and theoretical studies [41–47], the mechanism of this reaction has been controversial, even in the simple case of the reaction between butadiene and ethylene. In principle, two reaction mechanisms are possible, involving different transition state (TS) structures [46]: a concerted mechanism, where the two bonds in the TS are formed in one step either simultaneously (symmetric reaction path) or sequentially (asymmetric reaction path); or a stepwise mechanism that begins with the formation of a diradical or a zwitterion intermediate. The best evidence now indicates that a concerted path is favored in the reaction between butadiene and ethylene [47]. Diels–Alder addition of a diene on a Si(100) surface can also occur in principle by either concerted (symmetric or asymmetric) or stepwise mechanisms. Whereas most other adsorption reactions on Si(100) follow strongly asymmetric paths [48], orbital symmetry allows the Diels–Alder reaction to proceed on a symmetric reaction path. As shown in Fig. 3b, there is a positive overlap between the highest occupied molecular orbital (HOMO) of the surface and the lowest unoccupied molecular orbital (LUMO) of 1,3-cyclohexadiene. If this reaction occurs on a symmetric path, it will be the first known example of such a mechanism on Si(100).

We have performed a transition state search along the reaction path for the $[4_s+2_s]$ cycloaddition, exploring both concerted and stepwise mechanisms. Searches on symmetric (C_S) paths yield an apparent transition state on the concerted mechanism reaction hypersurface, though frequency analysis reveals this to be a second-order saddle point (SOSP) (Fig. 7). A SOSP is not a true transition state since there must be lower energy paths from reactants to products through a first-order saddle point. Nevertheless, this calculation establishes an upper bound to the energy of the true transition state. This SOSP is only 0.34 kcal mol^{-1} (B3LYP/6-31G**) higher then the energy of the separated, C_S-symmetric reactants. This number is small enough to suggest that there is no chemically significant barrier to the Diels–Alder reaction on a symmetric pathway. Although the C_S path is not the lowest-energy path, it is not kinetically forbidden, consistent with the expectation from orbital symmetry arguments.

However, several caveats must be applied in interpreting this calculation. While the theoretical methods used here are generally reliable, they may underestimate the activation barrier by as much as a few kcal mol^{-1}. Furthermore, in their lowest-

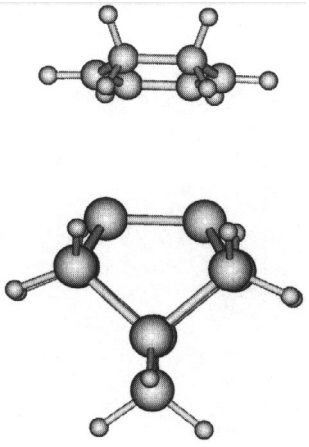

Fig. 7. Geometry of the second order transition state on the symmetric reaction pathway as calculated at the B3LYP/6-31G** level. The Si–C distance is 3.37 Å.

energy configuration, the dimers on the physical Si(100) surface are buckled rather than, symmetric. The small cluster model used here inherently underestimates the energy difference between buckled and symmetric dimers [21,49]. We can estimate the energy difference from calculations on larger clusters [21,49] or extended surfaces, [50–53] which indicate that buckled dimers are 2–4 kcal mol^{-1} lower in energy than symmetric dimers. Thus, the symmetric dimer SOSP is actually a few kcal mol^{-1} higher than the energy of the reactants when the surface is in its lowest energy surface structure, and searches restricted to symmetric reaction paths do not include the distortion energy required to symmetrize the dimer. Finally, the DFT methods used here fail to predict van der Waal's forces accurately. Neglect of dispersive forces may artificially raise the energy of weakly interacting complexes, like that at the symmetric saddle point. By neglecting the surface distortion energy and dispersive forces, our search along symmetric reaction paths makes two approximations which can each alter the apparent activation energy. However, the errors in these approximations are both small (each amounting to a few kcal mol^{-1}) and are in opposite directions. Accounting for these errors, we can estimate that the energy of the symmetric SOSP is no more than 4 kcal mol^{-1} higher than the lowest energy configuration of the isolated surface and diene. As noted above, there must be a lower energy asymmetric reaction path that does not go through the SOSP, so the true activation energy is still less than the estimate from the SOSP. Thus, if there is a barrier to the Diels–Alder reaction, it is only a few kcal mol^{-1}, and at room temperature it should not prevent the reaction from occuring at a useful rate. Nevertheless, if $[4_s+2_s]$ addition has even a small barrier, it may allow $[2_s+2_s]$ addition to compete kinetically. If surface distortion is required along the low energy reaction paths, then at reduced surface temperature, incident molecules are less likely to encounter the surface in a suitable configuration, which may prevent the Diels–Alder reaction. In fact, there is experimental evidence of a barrier to adsorption at low surface temperatures (see below).

There may also be low energy reaction paths that are strongly asymmetric. However, we were not able to locate a transition state or an intermediate with di-radical character along a stepwise mechanism reaction pathway. This is not to say that strongly asymmetric reaction paths are forbidden. Indeed, if the diene is placed in an asymmetric configuration at a distance above the surface where there are no significant chemical interactions, energy minimization leads directly to the Diels–Alder product through a concerted asymmetric path. However, we have not found evidence for a pathway with a metastable diradical intermediate.

3.2.3. 1,3-Butadiene and 2,3-dimethyl-1,3-butadiene

Several experiments have now verified the prediction that the Diels–Alder complex should be the dominant product of the reaction between a diene and the Si(100) surface. Teplyakov et al. [54,55] used multiple internal reflection infrared spectroscopy to determine that 1,3-butadiene and 2,3-dimethyl-1,3-butadiene react with the Si(100) surface to form the $[4_s+2_s]$ addition product. Hovis et al. [37] have applied infrared spectroscopy and scanning tunneling microscopy to the adsorption products of 1,3-butadiene and have found evidence that a small amount of the $[2_s+2_s]$ product is also formed. To make direct comparisons with these experiments, we have optimized $[4_s+2_s]$ and $[2_s+2_s]$ cycloaddition products of 1,3-butadiene and 2,3-dimethyl-1,3-butadiene on the Si(100) surface. Structural parameters and adsorption energies are presented in Tables 5 and 6, the optimized geometries of $[4_s+2_s]$ and $[2_s+2_s]$ 1,3-butadiene complexes are shown in Fig. 8, respectively. The two dienes adsorb in similar fashion, the $[4_s+2_s]$ product is thermodynamically more stable in both cases, by 25.6 kcal mol^{-1} (1,3-butadiene complex) and 28.8 kcal mol^{-1} (2,3-dimethyl-1,3-butadiene). Both the $[4_s+2_s]$ and $[2_s+2_s]$ complexes of 2,3-dimethyl-1,3-butadiene are slightly less stable than the corresponding complexes of the unsubstituted diene, as reflected in the lower adsorption energy (by 2.6 kcal mol^{-1} for the $[4_s+2_s]$ complex and by 5.8 kcal mol^{-1} for the $[2_s+2_s]$ complex) of the substituted diene. Note that the binding ener-

Table 5
Structural parameters and reaction energy for cycloaddition products of 1,3-butadiene on Si(100) surface as calculated at the B3LYP/6-31G* level

	$[4_s+2_s]$ complex	$[2_s+2_s]$ complex
Si–Si (Å)	2.375	2.366
Si–C (Å)	1.938	1.946, 1.979
C–C (Å)	3.101	1.563
Si–C–C (°)	109.3	100.1, 101.3
Si–Si–C (°)	100.8	77.3, 78.0
ΔE (kcal mol^{-1}) (B3LYP/6-31G*)	−67.5	−41.9

Table 6
Structural parameters and reaction energy for cycloaddition products 2,3-dimethyl-1,3-butadiene on Si(100) as calculated at the B3LYP/6-31G* level

	$[4_s+2_s]$ complex	$[2_s+2_s]$ complex
Si–Si (Å)	2.368	2.354
Si–C (Å)	1.935	1.945, 1.997
C–C (Å)	2.961	1.573
Si–C–C (°)	110.1	98.2, 120.5
Si–Si–C (°)	98.8	77.6, 78.1
ΔE (kcal mol^{-1}) (B3LYP/6-31G*)	−64.9	−36.1

gies here are given relative to the *cis* isomer of the butadiene. While the *trans* isomer is slightly more stable in the gas phase, the energy difference quoted is more directly comparable with that for cyclohexadiene. Moreover, the rate-limiting step in desorption would presumably be the formation of the *cis* isomer, so that the energies quoted should be a good estimate of desorption energies.

To help assign vibrational spectra, we have calculated vibrational frequencies of $[4_s+2_s]$ and $[2_s+2_s]$ complexes for both dienes. The calculated C–H stretch frequencies for 1,3-butadiene and 2,3-dimethyl-1,3-butadiene are reported in Tables 7 and 8, respectively. In each case the predicted vibrational spectra for the $[4_s+2_s]$ and $[2_s+2_s]$ products are clearly distinguishable, since the symmetric stretch of the vinylic CH_2 in the $[2_s+2_s]$ product (at 3048 cm^{-1}) occurs at much higher frequency than any of the modes in the $[4_s+2_s]$ product. Moreover, the experimental spectra [54,55] show excellent agreement with the predicted spectra for the $[4_s+2_s]$ product, confirming that the Diels–Alder complex is the dominant product of the reaction.

Near edge X-ray absorption fine structure (NEXAFS) measurements by Teplyakov et al. [55] on the absorption product of 2,3-dimethyl-1,

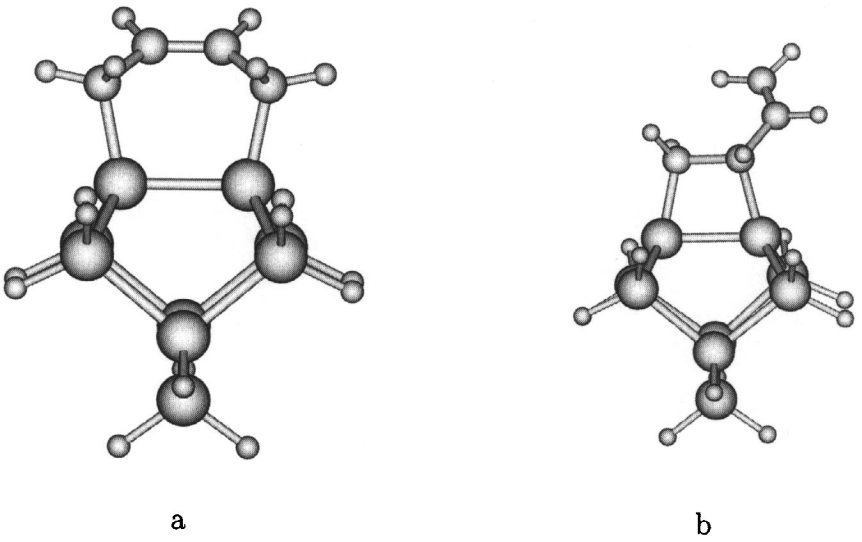

Fig. 8. Fully optimized geometry of (a) the product $[4_s+2_s]$ and (b) $[2_s+2_s]$ cycloaddition of 1,3-butadiene on the Si(100) surface as calculated at the B3LYP/6-31G** level.

Table 7
The calculated vibrational frequencies for the $[4_s+2_s]$ and $[2_s+2_s]$ cycloaddition adducts of 1,3-butadiene

	Group	Symmetry	Frequency (cm^{-1})
$[4_s+2_s]$			
	$-CH_2-$	s	2846
	$-CH_2-$	a	2853
	$-CH_2-$	a	2923
	$-CH_2-$	s	2923
	–CH–	a	2969
	–CH–	s	2989
$[2_s+2_s]$			
	$-CH_2-$	s	2834
	$-CH_2-$	a	2875
	–CH=		2922
	$=CH_2$		2941
	$-CH_2-$	s	2978
	$=CH_2$	a	3048

Table 8
The calculated vibrational frequencies for the $[4_s+2_s]$ and $[2_s+2_s]$ cycloaddition adducts of 2,3-dimethyl-1,3-butadiene

	Group	Symmetry	Frequency (cm^{-1})
$[4_s+2_s]$			
	$-CH_3$	a	2846
	$-CH_3$, $-CH_2-$	s	2847
	$-CH_3$, $-CH_2-$	s	2850
	$-CH_2-$	a	2854
	$-CH_3$	a	2885
	$-CH_3$	a	2885
	$-CH_3$	a	2916
	$-CH_2-$	s	2916
	$-CH_3$	a	2958
	$-CH_3$	s	2976
$[2_s+2_s]$			
	$-CH_3$	s	2849
	$-CH_3$	s	2853
	$-CH_2-$	s	2875
	$-CH_3$	a	2897
	$-CH_3$	a	2911
	$-CH_2-$	a	2925
	$-CH_3$	s	2940
	$-CH_3$	a	2944
	$=CH_2$	s	2982
	$=CH_2$	a	3054

3-butadiene indicate that the angle between the π orbitals and the surface normal is near 40°. In the predicted structure for the Diels–Alder product, the four carbon atoms in the ring lie in a plane that is tilted by 120° from the Si–C bonds. If we assume that the effective orientation of the π orbitals is perpendicular to the plane of the four carbon atoms in the Diels–Alder ring, and that the Si–C bond is parallel to the surface normal, then the angle of the π orbitals is predicted to be 30° from the surface normal. This is in reasonable agreement with the experiment, given the assumptions involved and the possibility that this angle is affected by interactions with adjacent dimers that are not included in the cluster model used here.

Teplyakov et al. [55] have shown that 2,3-dimethyl-1,3-butadiene does not chemisorb at 100 K (by either $[4_s+2_s]$ or $[2_s+2_s]$ addition) at a surface temperature of 100 K, though chemisorption occurs readily at 300 K. This is consistent with the suggestion above that some activation of surface modes is required for the Diels–Alder reaction. Moreover, this result indicates that $[2_s+2_s]$ addition of the diene is activated as well.

3.2.4. Benzene

Taguchi et al. [12] have observed that benzene chemisorbs on Si(100) at room temperature. They found two peaks in thermal desorption spectra which they assigned to species with approximate binding energies of -28 and -32 kcal mol^{-1}. Electron energy loss spectroscopy was consistent with a di-σ bonded configuration, and they proposed likely binding structures that can be described as $[4_s+2_s]$ and $[2_s+2_s]$ cycloaddition products. However, they could not distinguish between these possibilities. Two semiempirical studies have explored these and other proposed structures, and suggested that benzene may interact simultaneously with two surface dimers [56,57]. These calculations do not yield plausible binding energies or other direct comparisons with experiment. Recent work by Lopinski et al. [13] provides evidence from STM, infrared spectroscopy and semiempirical theory for a $[4_s+2_s]$ addition product on a single dimer and another, more stable product that interacts with two dimers. Finally, Gokhale et al. [14] have used thermal desorption spectroscopy, photoelectron spectroscopy and density functional theory to determine

that adsorbed benzene has the structure of the $[4_s+2_s]$ addition product.

To establish comparisons to the dienes described above, and to the calculations from other groups, we have optimized the geometries of $[4_s+2_s]$ and $[2_s+2_s]$ addition products of benzene on our single-dimer cluster model of Si(100), using the B3LYP functional and the 6-31G* basis. Again, the Diels–Alder product is the more stable, with a binding energy of -21.5 kcal mol^{-1}. These calculations employ a surface model with only one dimer, so interactions with an adjacent dimer are not included. The predicted binding energy of the $[4_s+2_s]$ product is lower than the estimated experimental binding energy, and the difference may be due to neglecting such interactions. Lopinski et al. predict a similar binding energy (-24.5 kcal mol^{-1}) for the $[4_s+2_s]$ product on a larger cluster, while Gokhale et al. find a binding energy of -32.2 kcal mol^{-1} on a larger cluster. The differences among these predicted binding energies reflect differences in theoretical approximations as well as differences in cluster size. We calculate that the $[2_s+2_s]$ product has a binding energy of only -4.7 kcal mol^{-1}, and is not likely to be important.

The difference in binding energy between the $[4_s+2_s]$ addition products of benzene and cyclohexadiene is about 32 kcal mol^{-1}. This is essentially the resonance energy in benzene, so it appears that the weak binding of benzene to the surface is simply a consequence of the aromatic stabilization in benzene. The difference in energy between the $[4_s+2_s]$ and $[2_s+2_s]$ addition products of benzene is 15.3 kcal mol^{-1}, which is close to the analogous difference for cyclohexadiene. Again, we attribute this difference to greater ring strain in the $[2_s+2_s]$ product.

3.3. Effects of post-hydrogenation

3.3.1. Hydrogenation of 1,3-cyclohexadiene adsorption complexes

Teplyakov et al. have studied the effect of exposing diene adducts to atomic hydrogen [55]. Infrared spectra of the post-hydrogenated 1,3-butadiene adduct show the presence of methyl groups on the surface. This observation would be consistent with reduction of the double bond in the $[2_s+2_s]$ adduct, but not the Diels–Alder product. This result is surprising, in light of the fact that the spectra prior to hydrogenation agree well with the predictions for the $[4_s+2_s]$ addition product and show no evidence of the terminal methylene characteristic of the $[2_s+2_s]$ product. To understand these observations, we have calculated the energy of species that are likely to be formed by hydrogenation of the adducts. Post-hydrogenation of the ethylene and acetylene $[2_s+2_s]$ addition products has been shown to produce Si–H bonds at low exposures [7,8]. By analogy, we expect the initial products formed by post-hydrogenation to be co-adsorption products of hydrogen with the cycloaddition adducts. We will show that hydrogen atoms can induce bond breaking and isomerization of the cycloaddition products even before the double bond is reduced.

We have fully optimized products of co-adsorption of the $[4_s+2_s]$ and $[2_s+2_s]$ adducts of 1,3-cyclohexadiene with two hydrogen atoms (Fig. 9). The calculated structural parameters of the co-adsorbate complexes are presented in Table 9. In both complexes, the Si–Si bond is broken after hydrogenation, relaxing to 4.73 and 3.89 Å in the $[4_s+2_s]$/2H and $[2_s+2_s]$/2H complex, respectively. The Si–Si distance in the $[4_s+2_s]$/2H complex is unreasonably long and the hydrogens bonded to the surface silicon atoms are rotated out, so as to be almost collinear with the axis connecting the two surface dimer atoms. This extreme relaxation clearly cannot happen on a real extended surface (the Si–Si distance on the unreconstructed surface is 3.84 Å) [29]. Thus, the energy of the $[4_s+2_s]$/2H complex is unrealistically low as a result of this over-relaxation of the small cluster model. Nevertheless, the $[2_s+2_s]$/2H complex is lower in energy (by 5.5 kcal mol^{-1}) than the $[4_s+2_s]$/2H complex and accounting for over-relaxation in the $[4_s+2_s]$/2H complex will increase the relative stability of the $[2_s+2_s]$/2H complex. Thus, while the $[4_s+2_s]$ Diels–Alder product is energetically favored as the initial product of diene adsorption, these calculations predict that post-hydrogenation will cause isomerization to the $[2_s+2_s]$/2H product.

We have also optimized products of co-adsorption of the $[4_s+2_s]$ and $[2_s+2_s]$ com-

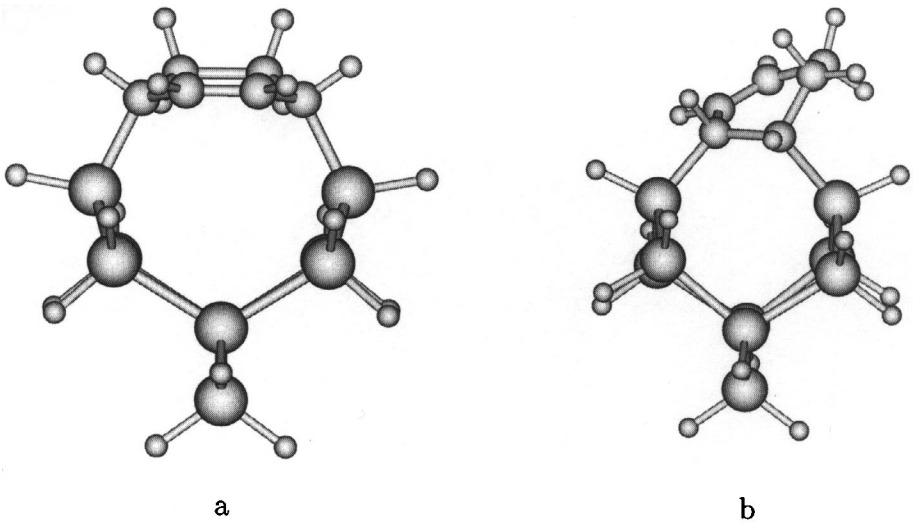

Fig. 9. Products of co-adsorption of two hydrogen atoms with cycloaddition products of 1,3-cyclohexadiene: (a) the $[4_s+2_s]$/2H complex; and (b) the $[2_s+2_s]$/2H complex, as calculated at the B3LYP/6-31G** level.

Table 9
Structural and energetic parameters for co-adsorption products of two H atoms with the $[4_s+2_s]$ and $[2_s+2_s]$ addition products of 1,3-cyclohexadiene, as calculated at the B3LYP/6-31G** level

	$[4_s+2_s]$/2H complex	$[2_s+2_s]$/2H complex
Si–Si (Å)	4.726	3.887
Si–C (Å)	1.952	1.946, 1.938
C–C (Å)	3.011[a]	1.555
Si–C–C (°)	116.5, 111.6	121.4
Si–C–H (°)	99.8	103.4, 99.2
Si–H (Å)	1.497	1.496
C–Si–H (°)	106.1	105.7, 104.1
ΔE_{rel} (kcal mol^{-1})	0.0	−5.5
ΔE_{rxn} (kcal mol^{-1})	−115.1	−135.8

The difference in total energy between the hydrogenated complexes (ΔE_{rel}) and the reaction energy for adding two H atoms to the initial cycloaddition product (ΔE_{rxn}) are reported.
[a] Distance across the ring, between the two carbons bonded to silicon atoms.

plexes with one hydrogen atom to understand the mechanism of the isomerization induced by hydrogenation. We have started from a fully optimized structure of the $[4_s+2_s]$ or $[2_s+2_s]$ adsorbate complex and added one hydrogen atom on the topmost silicon atom. Surprisingly, the two optimizations followed quite different paths. In the $[4_s+2_s]$/H complex, formation of a Si–H bond displaces a Si–C bond, resulting in a product with an intact dimer bond and a single Si–C bond (Fig. 10a, Table 10). On the other hand, in the $[2_s+2_s]$/H co-adsorbate complex, both Si–C bonds remain intact while the Si–Si dimer bond is cleaved, resulting in a di-σ bonded complex (Fig. 10b, Table 10). The di-σ bonded $[2_s+2_s]$/H complex is 10.2 kcal mol^{-1} higher in energy than the mono-σ bonded $[4_s+2_s]$/H complex. The reaction energies for addition of a hydrogen atom to the adsorbate complex are reported in Table 10. In both cases, formation of the hydrogenated surface radical intermediate has a strong energetic driving force in the presence of H atoms.

Based on these calculations, we propose the following mechanism for hydrogen-induced isomerization of a Diels–Alder adduct on Si(100). Fig. 11 illustrates the essential features of the mechanism in the case of 1,3-cyclohexadiene (for clarity, some additional isomers that are possible for the cyclohexadiene adduct are not shown; the species shown all have analogs in the butadiene adduct). Adsorption of the diene via the Diels–Alder mechanism forms a di-σ bonded $[4_s+2_s]$ complex (I). Adding the first hydrogen radical breaks one of the Si–C bonds in the $[4_s+2_s]$ complex. The resulting mono-σ radical complex has the resonance structures, II↔II′. The

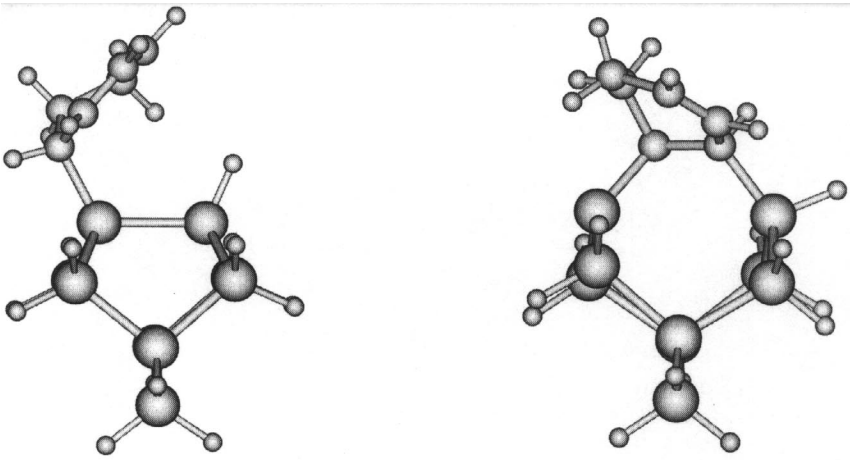

Fig. 10. Products of co-adsorption of one hydrogen atom with cycloaddition products of 1,3-cyclohexadiene: (a) the $[4_s+2_s]$/H complex; and (b) the $[2_s+2_s]$/H complex, as calculated at the B3LYP/6-31G** level.

Table 10
Structural and energetic parameters for co-adsorption products of one H atom with the $[4_s+2_s]$ and $[2_s+2_s]$ addition products of 1,3-cyclohexadiene, as calculated at the B3LYP/6-31G** level

	$[4_s+2_s]$/H complex	$[2_s+2_s]$/H complex
Si–Si (Å)	2.401	3.813
Si–C (Å)	1.954	1.946, 1.939
C–C (Å)	3.011[a]	1.556
Si–Si–C (°)	120.2, 115.2	120.4
Si–C–C (°)	117.6, 109.2	
Si–C–H (°)	102.5	102.9, 99.9
Si–H (Å)	1.491	1.498
C–Si–H (°)		104.0
ΔE_{rel} (kcal mol^{-1})	0.0	+10.2
ΔE_{rxn} (kcal mol^{-1})	−44.3	−49.4

The difference in total energy between the hydrogenated complexes (ΔE_{rel}) and the reaction energy for adding an H atom to the initial cycloaddition product (ΔE_{rxn}) are reported.
[a] Distance across the ring, between two carbons bonded to silicon atoms.

next hydrogen radical can add either to the cyclohexene radical in the mono-σ complex (Mechanism A, Fig. 11) or to the unhydrogenated surface atom (Mechanisms B, B′, Fig. 11). Mechanism A leads to the mono-σ bonded complex, III. Mechanism B results in the di-σ complex, IV, which is identical to the hydrogenated $[2_s+2_s]$ addition product. Our calculations show that each step in this mechanistic scheme is energetically favored. Since the Si–C bond in the $[4_s+2_s]$ complex breaks after hydrogenation, both the the $[4_s+2_s]$ and $[2_s+2_s]$ cycloaddition products can yield IV after post-hydrogenation. Thus, evidence for the presence of IV after post-hydrogenation does not imply that the $[2_s+2_s]$ product had been present before hydrogenation.

In fact, III is lower in energy than IV by 7.9 kcal mol^{-1}, so III is the thermodynamically preferred isomer. It may not be possible to distinguish III and IV by vibrational spectroscopy, and either product would be consistent with the currently available experimental results: post-hydrogenation of the 1,3-butadiene adduct produces vibrational spectra characteristic of CH_3 groups, but methyl groups would be present after reducing the butadiene analogs of either Ill or IV [15]. In any case, post-hydrogenation causes substantial isomerization which prevents it from being useful for distinguishing among isomers present before hydrogenation.

3.3.2. Hydrogenation of ethylene and acetylene adsorption complexes

It has previously been proposed that hydrogenation of ethylene and acetylene complexes on

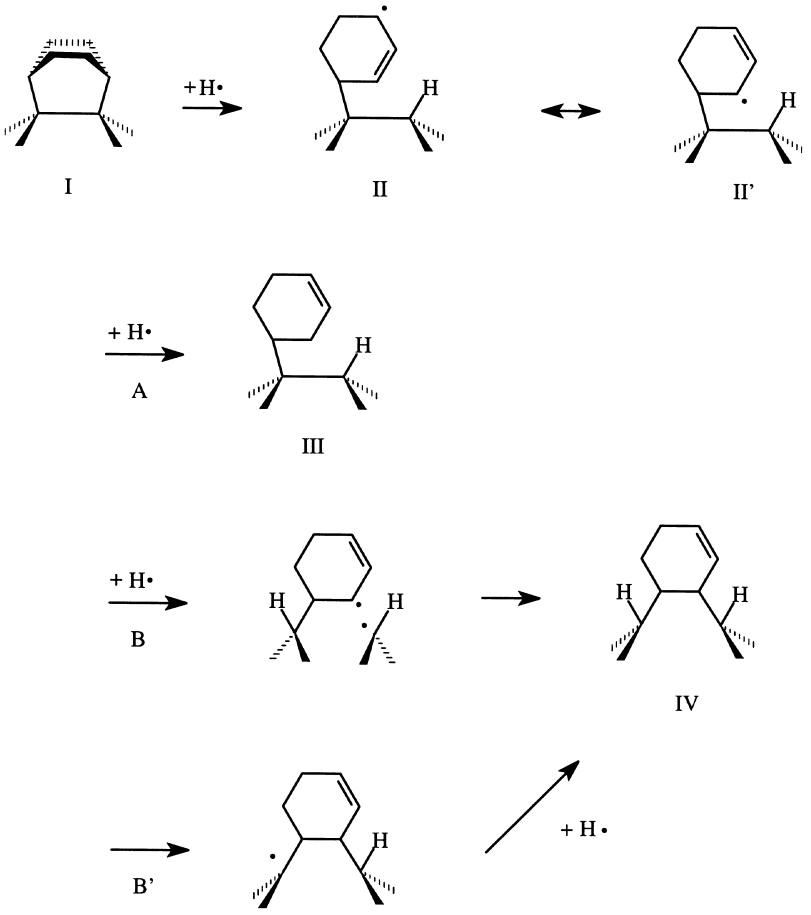

Fig. 11. Proposed mechanism for hydrogen-induced isomerization of a $[4_s+2_s]$ cycloaddition complex of a diene on the Si(100) surface. The mechanism is illustrated for the case of 1,3-cyclohexadiene, where some isomers are possible in addition to those shown. The isomers shown are those that have direct analogs in butadiene adducts.

Si(100) breaks the Si–Si dimer bond in those complexes [23,27,28]. To compare the mechanism of hydrogenation of the cycloaddition products to that of the ethylene and acetylene complexes, we have calculated the energies of these complexes with co-adsorbed hydrogen.

The optimized geometry of the co-adsorption product of ethylene with two H atoms (C_2H_4/2H) is shown on Fig. 12, with selected geometric parameters given in Table 11. The Si–Si dimer bond is cleaved after hydrogen adsorption, with the silicon–silicon distance being 3.91 Å. The carbon–carbon distance is essentially unchanged by hydrogen adsorption. Bond angles around the top-most silicon atoms are near the tetrahedral values. However, the Si–C–C angle (127.7°) is more distorted than in the ethylene adsorbate complex. Apparently, the energy gain from the favorable bond rearrangement of the top-most silicon atoms upon post-hydrogenation is partially compensated by unfavorable distortions in the carbon environment. The reaction energy for the co-adsorption of two H atoms per dimer is -138.0 kcal mol^{-1}, similar to the corresponding value for the $[2_s+2_s]$ addition product of cyclohexadiene.

The geometry of the hydrogenated acetylene complex (C_2H_4/2H) is similar to that of the corresponding ethylene complex. The structural data are reported in Table 11. The carbon–carbon bond

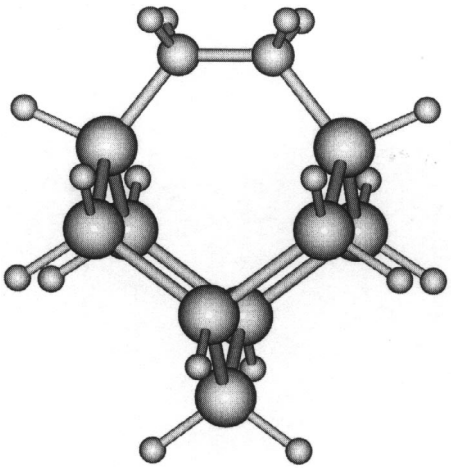

Fig. 12. B3LYP/6-31G* optimized geometry of product of co-adsorption of hydrogen and ethylene on the Si(100) surface.

Table 11
Structural parameters and reaction energy for the co-adsorption products of two H atoms with acetylene and ethylene on Si(100) surface, calculated at the B3LYP/6-31G* level

	$[4_s+2_s]$ complex	$[2_s+2_s]$ complex
Si–Si (Å)	3.905	3.936
Si–C (Å)	1.921	1.894
C–C (Å)	1.559	1.349
Si–C–C (°)	127.7	133.1
H–Si–C (°)	102.8	105.0
Si–Si–C=C (°)	2.1	0.0
ΔE_{rxn} (kcal mol^{-1})	−138.0	−142.6

The reaction energy for adding two H atoms to the initial cycloaddition product is also reported.

does not change upon co-adsorption and the Si–C–C angle is larger than that in the acetylene adsorbate complex (and larger than the optimal value of 120° for sp^2 hybridization). The reaction energy for post-adsorption of two H atoms per dimer is −142.6 kcal mol^{-1}.

As another attempt to estimate relative energies of adsorption complexes with a cleaved Si–Si dimer bond, we have calculated single point energies using the optimized geometries of the hydrogen co-adsorption products with the hydrogens removed. The ethylene and acetylene adsorption complexes with the silicon–silicon bond cleaved are 53.0 and 49.0 kcal mol^{-1}, respectively, higher than the structures with intact Si–Si dimer bonds. This further supports the assertion that the di-σ adsorption complexes with the Si–Si bond cleaved are not stable.

4. Conclusions

We have carried out a detailed study of $[2_s+2_s]$ and $[4_s+2_s]$ cycloadditions of several unsaturated hydrocarbons on the Si(100) surface. For 1,3-dienes or benzene, where both types of addition are possible, the $[4_s+2_s]$ product is consistently more stable than the $[2_s+2_s]$ product by 15–29 kcal mol^{-1}. The primary reason for the difference is the greater ring strain in the $[2_s+2_s]$ product. Substituents (as in 2,3-dimethyl-1, 3-butadiene) or constraints in the diene itself (as in 1,3-cyclohexadiene) play a secondary role in determining the relative energy of the two cycloaddition products. It may be possible to take advantage of such effects to enhance the selectivity for $[4_s+2_s]$ addition.

The differences in binding energy among the various $[2_s+2_s]$ addition products are primarily determined by the energy of the π-bond in the reactant. Acetylene binds more strongly than ethylene because the π-bond is weaker in acetylene; $[2_s+2_s]$ addition products of 1,3-dienes are more weakly bound than ethylene because the resonance energy in the diene is lost; benzene binds most weakly of all because it has the greatest resonance stabilization.

Experiments have shown that heating the adsorption products of acetylene or a butadiene results primarily in decomposition, while adsorbed ethylene and benzene desorb intact. The binding energies calculated here are consistently less favorable than −45 kcal mol^{-1} for adducts that desorb and more favorable than −50 kcal mol^{-1} for adducts that decompose. This suggests that the observed difference in chemical behavior is determined by simple competition between desorption and decomposition pathways, and that the barrier to decomposition is somewhat more than 45 kcal mol^{-1}.

We have located a second-order saddle point on the symmetric path leading to $[4_s+2_s]$ Diels–

Alder reaction. This saddle point is only 0.34 kcal mol^{-1} higher then the energy of reactants. We have not found any stable points along the stepwise mechanism pathway which are energetically higher than the energy of reactants. We conclude that the $[4_s+2_s]$ surface Diels–Alder reaction is at most weakly activated.

A mechanistic study of the post-hydrogenation of the 1,3-cyclohexadiene $[4_s+2_s]$ and $[2_s+2_s]$ cycloaddition products shows that exposure to atomic hydrogen causes dramatic isomerization. Both complexes can yield the same product after hydrogenation, so this reaction is not a useful tool for structural characterization.

Our calculations predict that the $[4_s+2_s]$ complex is the thermodynamic product of 1,3-diene adsorption on the Si(100) surface and that this product will be formed without significant kinetic limitations. We expect that dienes will generally undergo the Diels–Alder reaction on this surface, and on Ge(100) as well. These predictions have recently been experimentally confirmed by several groups. An important question for future work is whether kinetic competition with the $[2_s+2_s]$ may limit the selectivity of the reaction, and if so, whether substituent effects, annealing or other techniques can be used to enhance the yield of the $[4_s+2_s]$ product. We also look forward to efforts to exploit the double bond in the Diels–Alder product in further controlled reactions at the surface.

References

[1] H.N. Waltenburg, J.T. Yates, Jr, Chem. Rev. 95 (1995) 1589.
[2] M.J. Bozack, P.A. Taylor, W.J. Choyke, J.T. Yates, Jr, Surf. Sci. 177 (1986) L933.
[3] M. Nishijima, J. Yoshinobu, H. Tsuda, M. Onchi, Surf. Sci. 192 (1987) 383.
[4] L. Clemen, R.M. Wallace, P.A. Taylor, M.J. Dresser, W.J. Choyke, W.H. Weinberg, J.T. Yates, Jr, Surf. Sci. 268 (1992) 205.
[5] P.A. Taylor, R.M. Wallace, C.C. Cheng, W.H. Weinberg, M.J. Dresser, W.J. Choyke, J.T. Yates, Jr, J. Am. Chem. Soc. 114 (1992) 6754.
[6] J. Yoshinobu, H. Tsuda, M. Onchi, M.J. Nishijima, Chem. Phys. 87 (1987) 7332.
[7] W. Widdra, C. Huang, G.A.D. Briggs, W.H. Wienberg, J. Elect. Spectrosc. 64/65 (1993) 129.
[8] C. Huang, W. Widdra, W.H. Weinberg, Surf. Sci. 315 (1994) L953.
[9] W. Widdra, C. Huang, S.I. Yi, W.H. Weinberg, J. Chem. Phys. 105 (1996) 5605.
[10] R.J. Hamers, J.S. Hovis, S. Lee, H. Liu, J. Shan, J. Phys. Chem. B 101 (1997) 1489.
[11] J. Hovis, S. Lee, H. Liu, R.J. Hamers, J. Vac. Sci. Tech. A 15 (1997) 1153.
[12] Y. Taguchi, M. Fujisawa, T. Takaoka, T. Okada, M. Nishijima, J. Chem. Phys. 95 (1991) 6870.
[13] G.P. Lopinski, T. Fortier, D.J. Moffatt, R.A. Wolkow, J. Vac. Sci. Tech. A 16 (1998) 1037.
[14] S. Gokhale, P. Trischberger, D. Menzel, W. Widdra, H. Dröge, H.-P. Steinrück, U. Birkenheuer, U. Gutdeutsch, N. Rösch, J. Chem. Phys. 108 (1998) 5554.
[15] M.R. Linford, P. Fenter, P.M. Eisenberger, C.E.D. Chidsey, J. Am. Chem. Soc. 117 (1995) 3145.
[16] R. Konečný, D.J. Doren, J. Am. Chem. Soc. 119 (1997) 11098.
[17] C. Lee, W. Yang, R.G. Parr, Phys. Rev. B 37 (1988) 785.
[18] A.D. Becke, J. Chem. Phys. 98 (1993) 1372.
[19] M.J. Frisch, G.W. Trucks, H.B. Schlegel, P.M.W. Gill, B.G. Johnson, M.A. Robb, J.R. Cheeseman, T.A. Keith, G.A. Petersson, J.A. Montgomery, K. Raghavachari, M.A. Al-Laham, V.G. Zakrzewski, J.V. Ortiz, J.B. Foresman, J. Cioslowski, B.B. Stefanov, A. Nanayakkara, M. Challacombe, C.Y. Peng, P.Y. Ayala, W. Chen, M.W. Wong, J.L. Andres, E.S. Replogle, R. Gomperts, R.L. Martin, D.J. Fox, J.S. Binkley, D.J. Defrees, J. Baker, J.P. Stewart, M. Head-Gordon, C. Gonzales, J.A. Pople, Gaussian 94, Gaussian Inc., Pittsburgh, PA, 1995.
[20] P. Nachtigall, K.D. Jordan, K.C. Janda, J. Chem. Phys. 95 (1991) 8652.
[21] R. Konečný, D.J. Doren, J. Chem. Phys. 106 (1997) 2426.
[22] G. Rauhut, P. Pulay, J. Phys. Chem. 99 (1995) 3093.
[23] B.I. Craig, Surf. Sci. 329 (1995) 293.
[24] W. Widdra, C. Huang, W.H. Weinberg, Surf. Sci. 329 (1995) 295.
[25] Y. Imamura, Y. Morikawa, T. Yamasaki, H. Nakatsuji, Surf. Sci. 341 (1995) L1091.
[26] Q. Liu, R.J. Hoffmann, Am. Chem. Soc. 117 (1995) 4082.
[27] A.J. Fisher, P.E. Blöchl, G.A.D. Briggs, Surf. Sci. 374 (1997) 298.
[28] W. Pan, T. Zhu, W. Yang, J. Chem. Phys. 107 (1997) 3981.
[29] B.W. Holland, C.B. Duke, A. Paton, Surf. Sci. 140 (1984) L269.
[30] R.B. Woodward, R. Hoffmann, The Conservation of Orbital Symmetry, VCH, Weinheim, 1970.
[31] M. Weidenbruch, Coord. Chem. Rev. 130 (1994) 275.
[32] R. Okazaki, R. West, Adv. Organomet. Chem. 39 (1996) 231.
[33] M. Ishikawa, T. Fuchikami, M. Kumada, T. Higuchi, S. Miyamoto, J. Am. Chem. Soc. 101 (1979) 1348.
[34] J. Belzner, H. Ihmels, B.O. Kneisel, R. Herbst-Irmer, J. Chem. Soc., Chem. Comm. (1994) 1989.

[35] S.W. Benson, Thermochemical Kinetics, 2nd ed., Wiley, New York, 1976.
[36] R. Walsh, in: S. Patai, Z. Rappoport (Eds.), The Chemistry of Organic Silicon Compounds: Thermochemistry, Wiley, New York, 1989, p. 371.
[37] J. Hovis, H. Liu, R.J. Hamers, J. Chem. Phys. B 102 (1998) 6873.
[38] P.D. Barlett, K.E. Schueller, J. Am. Chem. Soc. 90 (1968) 6071.
[39] K.N. Houk, in: A.P. Marchand, R.E. Lehr (Eds.), Pericyclic Reactions, vol. 2, Academic, New York, 1977, p. 181.
[40] J. Sauer, R. Sustmann, Angew. Chem., Int. Edit. 19 (1980) 779.
[41] R.B. Woodward, T. Katz, Tetrahedron 5 (1959) 70.
[42] R.B. Woodward, R. Hoffmann, Angew. Chem., Int. Edit. 8 (1969) 781.
[43] M.J.S. Dewar, A.C. Griffin, S.J. Kirschner, J. Am. Chem. Soc. 96 (1974) 6225.
[44] M.J.S. Dewar, A.B. Pierini, J. Am. Chem. Soc. 106 (1984) 203.
[45] M.J.S. Dewar, S. Olivella, J.J.P. Stewart, J. Am. Chem. Soc. 108 (1986) 5771.
[46] K.N. Houk, J. González, Y. Li, Acc. Chem. Res. 28 (1995) 81.
[47] E. Goldstein, B. Beno, K.N. Houk, J. Am. Chem. Soc. 118 (1996) 6036.
[48] D. Doren, A.R. Brown, R. Konečný, Mat. Res. Soc. Symp. Proc. 448 (1997) 45.
[49] C. Yang, S.Y. Lee, H.C. Kang, J. Chem. Phys. 107 (1997) 3295.
[50] N. Roberts, R.J. Needs, Surf. Sci. 236 (1990) 112.
[51] J. Dąbrowski, M. Scheffler, Appl. Surf. Sci. 56–58 (1992) 15.
[52] J.E. Northrup, Phys. Rev. B 47 (1993) 10032.
[53] K. Inoue, Y. Morikawa, K. Terakura, M. Nakayma, Phys. Rev. B 49 (1994) 14774.
[54] A.V. Teplyakov, M.J. Kong, S.F. Bent, J. Am. Chem. Soc. 119 (1997) 11100.
[55] A.V. Teplyakov, M.J. Kong, S.F. Bent, J. Chem. Phys. 108 (1998) 4999.
[56] B.I. Craig, Surf. Sci. 280 (1993) L279.
[57] H.D. Jeong, S. Ryu, Y.S. Lee, S. Kim, Surf. Sci. 344 (1995) L1226.